Highly Localized Point-by-Point Fiber Bragg Grating for Multi-Parameter Measurement

Kaiming Yang, Bonan Liu, Changrui Liao, *Member, IEEE*, Yongxue Wang, Zhihao Cai, Jian Tang, Yatao Yang, and Yiping Wang, *Senior Member, IEEE, Senior Member, OSA*

***Abstract*—A three-parameter sensor based on a point-by-point fiber Bragg grating (PBP-FBG) is proposed. The fabricated sensor is 40 mm long. The spectrum loss at 1336.15 nm is selected to measure the surrounding liquid level. The sensitivity for liquid level sensing is −0.046 dB/mm. The temperature is measured using the Bragg dip shifts with sensitivity of 10.06 pm/ °C. The cut-off mode shift is used to measure the surrounding refractive index with sensitivity of 535.14 nm/RIU. As a benefit of femtosecond laser direct inscription fabrication, the grating length is controllable and the liquid level sensing range is expandable. This sensor provides a simple, reliable method for accurate liquid level, temperature and refractive index measurements in hazardous environments.**

***Index Terms*—Fiber Bragg gratings, fiber optics components, fiber optics sensors.**

I. Introduction

Monitoring of the liquid level, temperature and refractive index (RI) properties of surrounding media is of major significance in fields including chemical and biochemical processing, fuel storageand transportation systems, and wastewater treatment plants [1], [2]. Because of advantages that include corrosion resistance, electromagnetic interference resistance, high sensitivity and remote sensing capabilities, optical fiber sensors have been widely studied and applied [3]–[7]. The fiber Bragg grating (FBG) is among the most promising of these devices because it can maintain correct operation and information delivery in extreme surroundings, including conductive, hyperthermal, corrosive or explosive environments [8], [9]. With the aid of optical fiber post-processing techniques such as side polishing and chemical etching, use of FBGs in refractive index and liquid level measurement applications has become feasible [10], [11]. However, such post-processing will weaken the mechanical strength of the optical fiber while also increasing the manufacturing complexity. Khaliq demonstrated a long-period grating (LPG) liquid level sensor based on the RI difference between air and the liquid [12]. Although this LPG sensor can measure the surrounding RI directly using its cladding mode coupling mechanism, its multi-channel transmission capacity is limited by its wide bandwidth. The tilted FBG (TFBG) has attracted widespread attention because of the structure's high sensitivity to its surroundings caused by the high coupling efficiency of the cladding mode that occurs as a consequence of tilting the grating segments [2], 13]–[17]. The TFBG offers the advantages of both the FBG and the LPG. Tomasz et al. used the TFBG to realize simultaneous liquid level and temperature sensing [17]. Because of the different responses of the cladding modes and the core mode in the TFBG spectrum to changes in the liquid level and the temperature, both values can be measured independently. Qi et al. presented a fiber optic sensor for simultaneous measurement of the liquid level and the surrounding RI based on the TFBG [2]. However, the available length of the TFBG is subject to the length of the phase mask used in its fabrication. It is necessary to cascade multiple TFBGs to achieve a wide liquid level response range, which requires complex manufacturing and testing processes. However, in a manner similar to the tilted FBG, considerable enhancement of the cladding mode coupling strength is observed in highly localized point-by-point (PBP) FBGs with eccentricity, and PBP FBGs have thus been studied intensively for use as refractive index sensors [18]–[20]. The mechanism of cladding mode resonance enhancement of PBP-FBG has been theoretically analyzed and explained in references 20 and 21. The refractive index modulation region of highly localized PBP-FBG is much smaller than the core diameter, which is easy to cause the asymmetry of refractive index modulation, resulting in the increase of the overlapping integral of forward transmission core mode and reverse transmission cladding mode and the coupling efficiency is increased. So the cladding mode

Manuscript received June 18, 2021; revised August 4, 2021; accepted August 9, 2021. Date of publication August 11, 2021; date of current version October 18, 2021. This work was supported in part by the National Natural Science Foundation of China (NSFC) under Grants 62075136, 62005173, and 61805155, in part by the Natural Science Foundation of Guangdong Province under Grants 2018B030306003 and 2020A0505100066, and in part by the Science and Technology Innovation Commission of Shenzhen under Grants JCYJ20200109114001806 and RCYX20200714114524139. *(Corresponding authors: Changrui Liao; Yongxue Wang.)*

Kaiming Yang, Bonan Liu, Changrui Liao, Zhihao Cai, Jian Tang, and Yiping Wang are with the Key Laboratory of Optoelectronic Devices and Systems of Ministry of Education and Guangdong Province, College of Physics and Optoelectronic Engineering, Shenzhen University, Shenzhen, Guangdong 518060, China, and also with the Shenzhen Key Laboratory of Photonics Devices and Sensing Systems for Internet of Things, Guangdong and Hong Kong Joint Research Centre for Optical Fiber Sensors, Shenzhen University, Shenzhen, Guangdong 518060, China (e-mail: yangkaiming@email.szu.edu.cn; ssamliu@163.com; cliao@szu.edu.cn; 2060453003@email.szu.edu.cn; tangjian2@email.szu.edu.cn; ypwang@szu.edu.cn).

Yongxue Wang is with the School of Electronic and Communication Engineering, Shenzhen Polytechnic, Shenzhen, Guangdong 518060, China (e-mail: wangyongxue@szpt.edu.cn).

Yatao Yang is with the College of Electronics and Information Engineering, Shenzhen University, Shenzhen, Guangdong 518060, China (e-mail: yatao86@163.com).

Color versions of one or more figures in this article are available at https://doi.org/10.1109/JLT.2021.3104102.

Digital Object Identifier 10.1109/JLT.2021.3104102

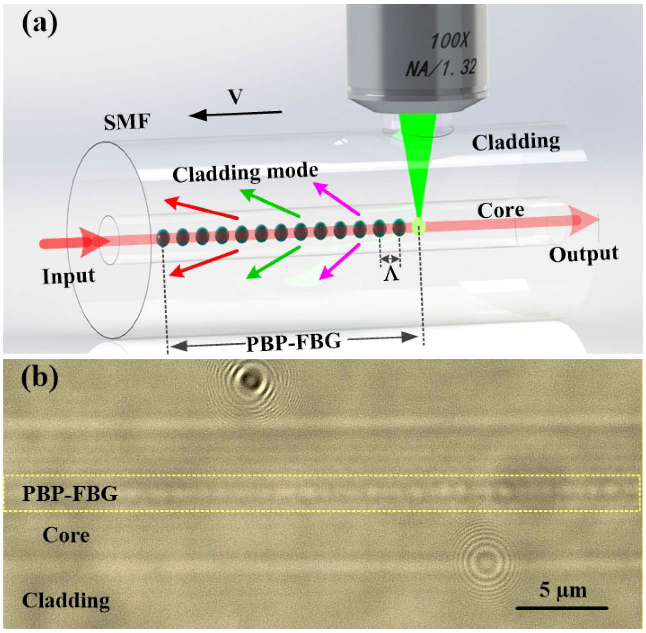

Fig. 1. (a) Schematic of PBP FBG machining process. (b) Optical microscope photograph of a PBP FBG.

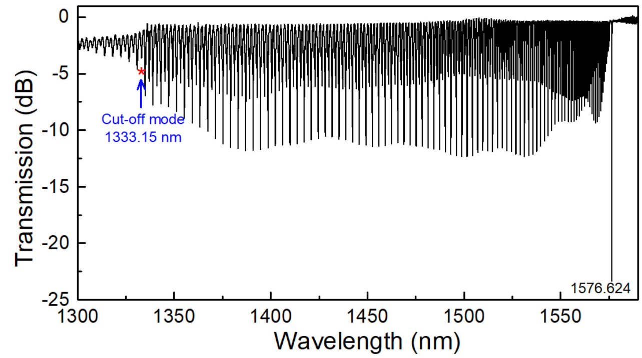

Fig. 2. Spectrum of the fabricated PBP FBG.

resonance is significantly enhanced. Like the tilted FBG, it is therefore reasonable to infer that by appropriate use of the highly localized PBP FBG's sensitivity to temperature, refractive index and immersion changes, it is possible to measure these quantities accurately. When compared with the TFBG, the PBP FBG can be longer and a wider liquid level sensing range can thus be realized.

In this study, a highly localized PBP FBG is proposed to perform three-parameter sensing of the liquid level, RI and temperature. Introduction of the localization effect caused major enhancement of the cladding mode resonance of the FBG. The sensing principle is based on the fact that when the FBG is surrounded by a liquid, its cladding mode resonance responds to changes in the liquid level or the liquid's RI, while the Bragg resonance is mainly sensitive to the temperature. The FBG was fabricated by femtosecond laser PBP direct writing. This method realizes length-controllable fabrication that breaks through the phase mask length limitation. A wide liquid level sensing range is also achieved.

II. Highly Localized PBP FBG Inscription

The fs laser PBP direct writing experimental setup illustrated in Fig. 1 and described in [21] was used to inscribe the PBP FBG. The fs laser amplifier (PH1-10, Light Conversion, Lithuania) emitted laser pulses at a center wavelength of 513 nm with pulse duration of 250 fs at a repetition rate of 200 kHz. The pulse energy was 35 nJ and this energy was controlled precisely using an attenuator consisting of a half-wave plate and a Glan prism. The laser spot size undergoes expansion via a beam expander, after which the spot diameter exceeds 10 mm. The pulses were focused into a single-mode fiber (SMF; Corning SMF-28) through an oil-immersed 100× objective lens (numerical aperture (NA) = 1.32). The fiber was stripped and mounted on a three-axis translation stage (Aerotech) that was controlled via a computer to ensure precise motion control during fabrication. Using the PBP direct inscription, the fiber was moved along its axial direction to inscribe RI perturbation points with a constant period of Λ, which allows grating pitch and length controllability to be achieved. In this work, the grating pitch was configured to be 545 nm in advance, thus yielding a first-order FBG with Bragg resonance at 1576.624 nm. The length of this FBG is 40 mm.

The transmission spectrum was measured using an amplified spontaneous emission (ASE) light source and an optical spectrum analyzer (OSA). A fiber polarizer and a polarization controller were also set up to secure linear polarization. Figure 2 depicts the spectrum of the PBP FBG. This spectrum shows that the Bragg resonance intensity reaches −20 dB, while the cladding mode resonance intensity is approximately −10 dB. The bandwidth of the Bragg resonance is as narrow as 0.1 nm. The insertion loss on the longer wavelength side is less than 0.01 dB. A wide cladding mode resonance range in the shorter wavelength direction of the Bragg resonance can also be observed, covering the range from the cut-off wavelength of 1333.15 nm to the Bragg wavelength. The cladding mode resonance was enhanced as a consequence of the strong localization effect caused by the small RI modulation area, which only covers a small fraction of the fiber core [20], [21]. Note here that it is not necessary for this type of FBG to be eccentric to be able to guarantee both a strong Bragg resonance and low insertion loss simultaneously.

III. Sensing Test of Highly Localized PBP FBG

The liquid level sensing performance of the fabricated FBG was investigated. The experimental setup used is illustrated in Fig. 3. As shown, the FBG was placed vertically into a beaker and the hole in the bottom of the beaker that allowed the optical fiber to pass through was sealed using glue. Visible red laser light was then launched into the fiber to locate the FBG to secure quantitative coverage of the liquid level. Water (RI = 1.33) was then injected into the beaker and the spectrum was recorded as the water level increased. Fig. 4(a) shows the

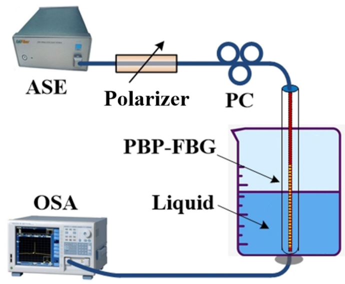

Fig. 3. Schematic diagram of the liquid level test setup.

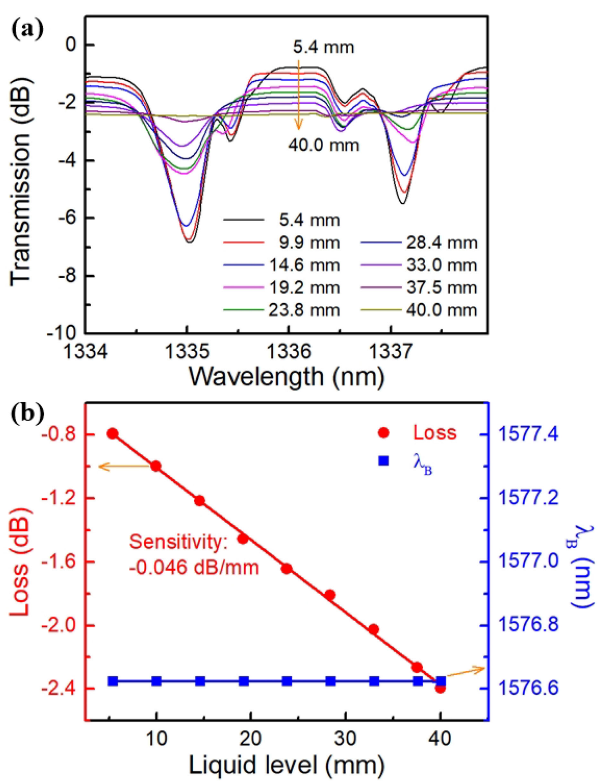

Fig. 4. (a) Spectrum evolution of the FBG with respect to the liquid level near 1336 nm. (b) Correlation of the loss with the liquid level around 1336.15 nm (red line) and correlation of the Bragg wavelength and the liquid level (blue line).

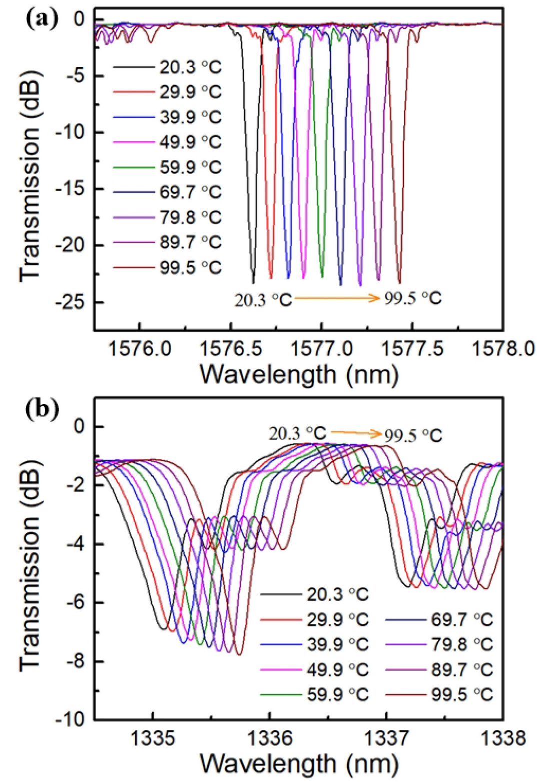

Fig. 5. (a) The shift of Bragg wavelength with the temperature and (b) the shift of the cladding mode resonance with the temperature near 1336nm.

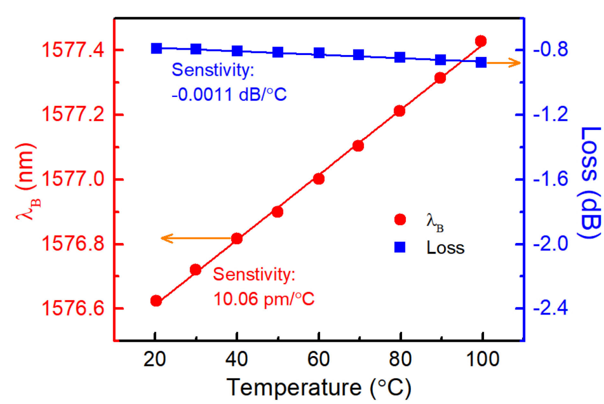

Fig. 6. Correlation of the loss with the SRI around 1336.15 nm (blue line) and correlation of the Bragg wavelength and the SRI (red line).

evolution of the cladding mode spectrum near 1336 nm. As the water level increased, both the intensity of the cladding mode resonance and the transmission loss in the flat area between the two cladding mode resonances around 1336.15 nm varied. After further investigation, it was found that the correlation of the cladding mode resonance with the liquid level is not linear or regular. The loss around 1336.15 nm was thus selected to observe the liquid level sensing performance. As shown in Fig. 4(b), the loss changes linearly with changes in the water level with sensitivity of −0.046 dB/mm. Fig. 4(b) also shows that the Bragg dip remains virtually unchanged versus the liquid level.

The thermal response of the fabricated PBP FBG was evaluated by placing the FBG into a temperature-controlled oven. As the temperature increased from 20.3 °C to 99.5 °C, the transmission spectrum was recorded at each increment of approximately 10 °C. Figs. 5(a) and 5(b) depict the shifts in the Bragg dip and in the cladding mode in the vicinity of 1336 nm, respectively. The Bragg dip is observed to shift toward longer wavelengths. As shown in Fig. 6, the dip responses vary linearly and the temperature sensitivity is 10.06 pm/°C. Additionally, the spectral evolution of the flat area between the two cladding mode resonances around 1336.15 nm was also studied and the results are shown in Fig. 6. The loss remains virtually unchanged, with sensitivity of −0.0011 dB/°C. When combined with the temperature response of the Bragg dip, the cross-sensitivity

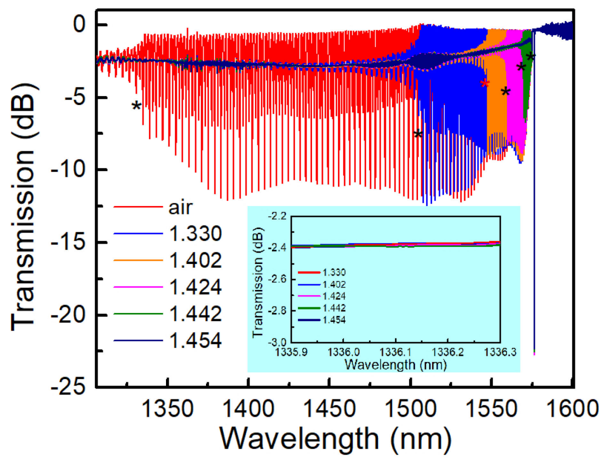

Fig. 7. Spectral evolution of the PBP FBG in different RI liquids; Inset: The spectrum around 1336 nm.

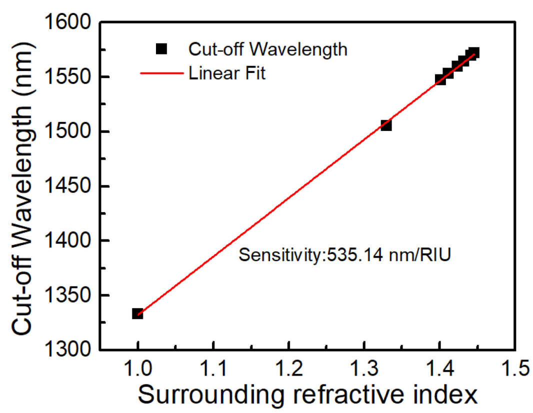

Fig. 8. The linear correlation between the SRI and the cut-off wavelength of the PBP FBG.

between the temperature and the liquid level can be compensated to realize simultaneous dual-parameter sensing.

Additionally, under the condition of being fully covered by liquids, surrounding RI (SRI) sensing can be performed. The SRI response of the PBP FBG has been examined by immersing the FBG into a series of RI matching oils. The results are shown in Fig. 7. The cut-off wavelength is shown to shift toward longer wavelengths, which indicates that when the SRI increased, more of the cladding modes leaked from the fiber because their effective RI was lower than the external RI. The linear correlation between the SRI and the cut-off wavelength is shown in Fig. 8, where the corresponding sensitivity is calculated to be 535.14 nm/RIU. In addition, the measurable RI range extends from 1 to 1.454 as a benefit of the wide bandwidth of the cladding mode resonance.

It can also be seen in Fig. 7 that the losses corresponding to the different SRIs at 1336.15 nm all have the same value (see the inset of Fig. 7), which indicates that when liquids with different RIs cover the FBG fully, the corresponding losses are the same. Such a loss indicates the end of the liquid level test. Because the FBG was surrounded by air at the start of the liquid level test, it can be deduced that the losses at the start and the end of the liquid level test are not relevant to the SRI. Therefore, the SRI will not affect the liquid level sensing result if the loss at 1336.15 nm is selected. The response of the Bragg dip to changes in the SRI can be neglected because the Bragg dip mainly responds to the surrounding temperature. The cladding mode resonance dip shifts in almost the same manner to the Bragg dip. As a result, the Bragg dip shift can be used to compensate the sensing results to eliminate the cross-sensitivity between the SRI and the temperature. All cross-sensitivity has thus been removed and three-parameter sensing is realized.

IV. Conclusion

We proposed a three-parameter sensor based on a PBP-FBG. The length of this sensor is 40 mm. The liquid level is measured based on the spectrum loss around 1336.15 nm. The sensitivity for liquid level sensing is -0.046 dB/mm. The temperature sensing was performed based on the drift of the Bragg dip, with sensitivity of 10.06 pm/°C. The sensing of temperature and liquid level can be performed simultaneously. The drift of the cut-off wavelength is used to measure the SRI, with sensitivity of 535.14 nm/RIU. All cross-sensitivities have been effectively removed. This study provides a simple and reliable method for accurate liquid level, temperature and refractive index measurements that can be applied in hazardous environments. When compared with the traditional TFBG, the manufacture of the proposed PBP-FBG sensor is not limited by the phase mask length, which enables expansion of the liquid level measurement range.

References

[1] C. A. R. Diaz *et al.*, "Optical fiber sensing for sub-millimeter liquid-level monitoring: A review," *IEEE Sens. J.*, vol. 19, no. 17, pp. 7179–7191, Sep. 2019.

[2] Q. Jiang, D. Hu, and M. Yang, "Simultaneous measurement of liquid level and surrounding refractive index using tilted fiber Bragg grating," *Sensor Actuators A-Phys.*, vol. 170, no. 1/2, pp. 62–65, Nov. 2011.

[3] Y. Wang, "Review of long period fiber gratings written by CO_2 laser," *J. Appl. Phys.*, vol. 108, no. 8, pp. 081101-1–081101-18, Oct. 2010.

[4] F. Chiavaioli and D. Janner, "Fiber optic sensing with lossy mode resonances: Applications and perspectives," *J. Lightw. Technol.*, vol. 39, no. 12, pp. 3855–3870, Jun. 2021.

[5] F. Chiavaioli *et al.*, "Femtomolar detection by nanocoated fiber label-free biosensors," *ACS Sensors*, vol. 3, no. 5, pp. 936–943, May 2018.

[6] F. Chiavaioli, F. Baldini, S. Tombelli, C. Trono, and A. Giannetti, "Biosensing with optical fiber gratings," *Nanophotonics-Berlin*, vol. 6, no. 4, pp. 663–679, Jul. 2017.

[7] Z. Li, X. Yang, H. Zhu, and F. Chiavaioli, "Sensing performance of fiber-optic combs tuned by nanometric films: New insights and limits," *IEEE Sens. J.*, vol. 21, no. 12, pp. 13305–13315, Jun. 2021.

[8] N. Jovanovic, A. Fuerbach, G. D. Marshall, M. Ams, and M. J. Withford, "Fibre grating inscription and applications," in *Femtosecond Laser Micromaching: Photonic Microfluidic Devices Transparent Material*, R. Osellame, G. Cerullo, and R. Ramponi Eds., Berlin, Germany: Springer, 2012, pp. 197–225.

[9] C. Lin *et al.*, "Fiber surface Bragg grating waveguide for refractive index measurements," *Opt. Lett.*, vol. 42, no. 9, pp. 1684–1687, 2017.

[10] N. Chen, B. F. Yun, and Y. P. Cui, "Cladding mode resonances of etch-eroded fiber Bragg grating for ambient refractive index sensing," *Appl. Phys. Lett.*, vol. 88, no. 13, pp. 133902-1–133902-3, Mar. 2006.

[11] C. Liao *et al.*, "D-shaped fiber grating refractive index sensor induced by an ultrashort pulse laser," *Appl. Opt.*, vol. 55, no. 7, 2016, Art. no. 1525.

[12] S. Khaliq, S. W. James, and R. P. Tatam, "Fiber-optic liquid-level sensor using a long-period grating," *Opt. Lett.,* vol. 26, no. 16, pp. 1224–1226, Aug. 2001.

[13] J. Albert, L.-Y. Shao, and C. Caucheteur, "Tilted fiber Bragg grating sensors," *Laser Photon. Rev.,* vol. 7, no. 1, pp. 83–108, 2013.

[14] C. Mou, K. Zhou, Z. Yan, H. Fu, and L. Zhang, "Liquid level sensor based on an excessively tilted fibre grating," *Opt. Commun.,* vol. 305, pp. 271–275, Sep. 2013.

[15] A. F. Obaton, G. Laffont, C. Wang, A. Allard, and P. Ferdinand, "Tilted fibre bragg gratings and phase sensitive-optical low coherence interferometry for refractometry and liquid level sensing," *Sensor Actuators A-Phys.,* vol. 189, pp. 451–458, Jan. 2013.

[16] T. Guo, F. Liu, B.-O. Guan, and J. Albert, "INVITED Tilted fiber grating mechanical and biochemical sensors," *Opt. Laser Technol.,* vol. 78, pp. 19–33, Apr. 2016.

[17] T. Osuch, T. Jurek, K. Markowski, and K. Jedrzejewski, "Simultaneous measurement of liquid level and temperature using tilted fiber Bragg grating," *IEEE Sens. J.,* vol. 16, no. 5, pp. 1205–1209, Mar. 2016.

[18] H. Chikh-Bled, M. Debbal, M. Chikh-Bled, C.-E. Quadah, V. Calero-Vila, and M. Bouregaa, "Refractive index sensor in eccentric fiber Bragg gratings using a point-by-point IR femtosecond laser," *Appl. Opt.,* vol. 58, no. 3, pp. 528–534, Jan. 2019.

[19] K. Chah, V. Voisin, D. Kinet, and C. Caucheteur, "Surface plasmon resonance in eccentric femtosecond-laser-induced fiber Bragg gratings," *Opt. Lett.,* vol. 39, no. 24, pp. 6887–6890, Dec. 2014.

[20] J. Thomas *et al.*, "Cladding mode coupling in highly localized fiber Bragg gratings: Modal properties and transmission spectra," *Opt. Exp.,* vol. 19, no. 1, pp. 325–341, Jan. 3, 2011.

[21] J. U. Thomas *et al.*, "Cladding mode coupling in highly localized fiber Bragg gratings II: Complete vectorial analysis," *Opt. Exp.,* vol. 20, no. 19, pp. 21434–21449, Sep. 2012.

[22] K. Yang, C. Liao, S. Liu, J. He, J. Wang, and Y. Wang, "Optical fiber tag based on an encoded fiber Bragg grating fabricated by femtosecond laser," *J. Lightw. Technol.,* vol. 38, no. 6, pp. 1474–1479, 2020.

Kaiming Yang received the B.S. degree in optical information science and technology from East China JiaoTong University, Nanchang, China, in 2012 and the Ph.D. degree in optical engineering from Shenzhen University, Shenzhen, China, in 2019. He is currently a Postdoctoral Researcher with Shenzhen University. His current research interests include fiber Bragg gratings and femtosecond laser micromachining.

Bonan Liu received the B.S. degree in optical information engineering from Shenzhen University, Shenzhen, China, in 2016 and the master's degree in telecommunication engineering from the University of New South Wales, Sydney, NSW, Australia, in 2019. He is currently working toward the Ph.D. degree with Shenzhen University. His current research interests include tilted fiber gratings and fiber micro cavity.

Changrui Liao (Member, IEEE) received the B.Eng. degree in optical engineering and the M.S. degree in physical electronics from the Huazhong University of Science and Technology, Wuhan, China, in 2005 and 2007, respectively, and the Ph.D. degree in electrical engineering from Hong Kong Polytechnic University, Hong Kong, in 2012. He is currently with Shenzhen University, Shenzhen, China, as an Associate Professor. His current research interests include femtosecond laser micromachining, optical fiber sensors, and opto-microfluidics.

Yongxue Wang biography not available at the time of publication.

Zhihao Cai received the B.S. degree in measurement and control technology and instruments from Shenzhen University, Shenzhen, China, in 2020. He is currently a Postgraduate Student in optical engineering with Shenzhen University. His current research interests include fiber gratings and femtosecond laser micromachining.

Jian Tang biography not available at the time of publication.

Yatao Yang biography not available at the time of publication.

Yiping Wang (Senior Member, IEEE) received the B.Eng. degree in precision instrument engineering from the Xi'an Institute of Technology, Xi'an, China, in 1995, and the M.S. and Ph.D. degrees in optical engineering from Chongqing University, Chongqing , China, in 2000 and 2003, respectively. From 2003 to 2005, he was with Shanghai Jiao Tong University, Shanghai, China, as a Postdoctoral Fellow. From 2005 to 2007, he was with Hong Kong Polytechnic University, Hong Kong, as a Postdoctoral Fellow. From 2007 to 2009, he was with the Institute of Photonic Technology (IPHT), Jena, Germany, as a Humboldt Research Fellow. From 2009 to 2011, he was with the Optoelectronics Research Centre (ORC), University of Southampton, U.K., as a Marie Curie Fellow. Since 2012, he has been with Shenzhen University, Shenzhen, China, as a Distinguished Professor. He has authored or coauthored one book, 21 patent applications, and more than 280 journal and conference papers. His current research interests include optical fiber sensors, fiber gratings, and photonic crystal fibers. Prof. Wang is a Senior Member of the Optical Society of America, and the Chinese Optical Society.